Variability and Trends of Air Temperature and Pressure in the Maritime Arctic, 1875–2000

Igor V. Polyakov,* Roman V. Bekryaev,*[+] Genrikh V. Alekseev,[+] Uma S. Bhatt,*
Roger L. Colony,* Mark A. Johnson,[#] Alexander P. Maskshtas,* and David Walsh*

*International Arctic Research Center, University of Alaska Fairbanks, Fairbanks, Alaska
[+]Arctic and Antarctic Research Institute, St. Petersburg, Russia
[#]Institute of Marine Science, University of Alaska Fairbanks, Fairbanks, Alaska

ABSTRACT

Arctic atmospheric variability during the industrial era (1875–2000) is assessed using spatially averaged surface air temperature (SAT) and sea level pressure (SLP) records. Air temperature and pressure display strong multidecadal variability on timescales of 50–80 yr [termed low-frequency oscillation (LFO)]. Associated with this variability, the Arctic SAT record shows two maxima: in the 1930s–40s and in recent decades, with two colder periods in between. In contrast to the global and hemispheric temperature, the maritime Arctic temperature was higher in the late 1930s through the early 1940s than in the 1990s. Incomplete sampling of large-amplitude multidecadal fluctuations results in oscillatory Arctic SAT trends. For example, the Arctic SAT trend since 1875 is $0.09 \pm 0.03°C$ decade^{-1}, with stronger spring- and wintertime warming; during the twentieth century (when positive and negative phases of the LFO nearly offset each other) the Arctic temperature increase is $0.05 \pm 0.04°C$ decade^{-1}, similar to the Northern Hemispheric trend ($0.06°C$ decade^{-1}). Thus, the large-amplitude multidecadal climate variability impacting the maritime Arctic may confound the detection of the true underlying climate trend over the past century. LFO-modulated trends for short records are not indicative of the long-term behavior of the Arctic climate system. The accelerated warming and a shift of the atmospheric pressure pattern from anticyclonic to cyclonic in recent decades can be attributed to a positive LFO phase. It is speculated that this LFO-driven shift was crucial to the recent reduction in Arctic ice cover. Joint examination of air temperature and pressure records suggests that peaks in temperature associated with the LFO follow pressure minima after 5–15 yr. Elucidating the mechanisms behind this relationship will be critical to understanding the complex nature of low-frequency variability.

1. Introduction

An analysis of observational records shows that the global surface air temperature (SAT) has increased by 0.6°C since 1861, with a slightly higher rate of warming in the twentieth century (Jones et al. 1999). During that period, the 1990s were the warmest decade in the Northern Hemisphere. This warming was associated with an increase in land surface precipitation, a decrease in snow cover and sea ice extent, sea level rise, and changes in the atmospheric and oceanic circulation patterns (Houghton et al. 2001). Emissions of anthropogenic greenhouse gases, which have increased by 10%–50% since the beginning of the industrial era, may drive substantial changes in the climate system. Using 400 yr of proxy data, Overpeck et al. (1997) suggested that before 1920 volcanic aerosol loading and solar radiation were major contributors to Arctic SAT change, but that after 1920 increasing greenhouse gas concentrations dominated Arctic air temperature variability.

The ocean–atmosphere system exhibits natural variability in the North Atlantic sector at multidecadal timescales, as seen in the paleoclimate record (Delworth and Mann 2000) as well as diagnosis of slow thermohaline circulation changes in coupled climate model simulations (Delworth et al. 1993; Timmerman et al. 1998). Strikingly similar low-frequency variability in the ocean–atmosphere system is also excited by solar variability (Cubasch et al. 1997; Waple et al. 2002) and greenhouse gas forcing (Delworth and Knutson 2000). Shindell et al. (2001) identified multidecadal variability in the North Atlantic in a study that forced an atmospheric GCM coupled to a mixed layer ocean with observed solar and ozone fluctuations. In nature, it is likely that a variety of forcing can excite these modes of low-frequency variability. In addition, it is expected that the climate response to increasing greenhouse gases projects on this multidecadal variability (Stott et al. 2000; Crowley 2000), leading to changes in amplitude and frequency.

Corresponding author address: Dr. Igor Polyakov, International Arctic Research Center, University of Alaska Fairbanks, P.O. Box 757335, Fairbanks, AK 99775.
E-mail: igor@iarc.uaf.edu

General circulation models predict enhanced high-latitude warming due to positive feedbacks such as the ice–albedo feedback, where warming leads to a reduction of ice and snow coverage decreasing albedo and resulting in further snow and sea ice retreat (Cess et al. 1991; Manabe and Stouffer 1994). However, Walsh and Crane (1992) found substantial biases in present-day simulations of Arctic surface air temperature and sea level pressure (SLP) from five general circulation models when compared with observations. The largest uncertainty in modeling Arctic climate arises from clouds, and their response to changes in radiation and albedo (Gates et al. 1996). The implications that these model-to-model differences have for the simulation of realistic Arctic climate change and variability may be significant.

Spectacular changes have occurred in the Arctic over the last few decades. Arctic SAT shows warming (Martin et al. 1997; Rigor et al. 2000). In the late 1980s through the early 1990s, SLP decreased and the cyclonic vorticity of winds increased to extreme values relative to any time in the past several decades (Walsh et al. 1996). The number of cyclones penetrating into the Arctic from the North Atlantic has increased (Serreze et al. 1997). Concurrent with these atmospheric changes are reductions in Arctic ice extent (Parkinson et al. 1999) and a decrease of ice thickness in the central Arctic (Rothrock et al. 1999). Observations reveal a significant salinification of the surface water in the mid-Eurasian Basin and a retreat of the Arctic cold halocline (Steele and Boyd 1998). According to Johnson and Polyakov (2001), this was due to the eastward diversion of Russian rivers' discharge in response to the anomalous atmospheric circulation and also due to enhanced ice production and brine rejection in the Laptev Sea.

Despite the significant body of research and a preliminary understanding of driving mechanisms of the recent observed changes in the Arctic, there is still a large degree of uncertainty about the role of natural low-frequency variability and trends. The goal of this research is to assess long-term (century plus) Arctic air temperature and pressure trends and their low-frequency variability using available observational data from around the entire Arctic. Two composite monthly time series, one for SAT and another for SLP for the area poleward of 62°N elucidate the Arctic and sub-Arctic atmospheric variability. Long-term Arctic observations are now available due to recently released Russian meteorological observations from coastal stations and manned North Pole (NP) drifting stations. These newly available data, pooled with other datasets, offer the possibility for new insights into trends and variability of the Arctic atmosphere, and recently observed changes in the Arctic environment.

2. Data

The datasets of monthly surface air temperature and sea level pressure used in this study contain data from land stations, Russian NP stations, and drifting buoys operated by the International Arctic Buoy Programme (IABP). Several databases are consolidated. The Arctic and Antarctic Research Institute (AARI) produced an extensive archive of SAT and SLP observations at Russian land stations (V. F. Radionov 2001, personal communication; Aleksandrov and Dementyev 1995). The first high-latitude Russian stations appeared in the late nineteenth century and early twentieth century and rapidly increased in number in the 1930s–40s. The Earth Observing System (EOS) Distributed Active Archive Center (DAAC) at the National Snow and Ice Data Center (NSIDC), the University of Colorado, the Meteorological Service of Canada, and the National Aeronautics and Space Administration (NASA) Goddard Institute for Space Studies provided monthly air temperatures for Europe, Greenland, the Canadian Northwest Territories, and Alaska. The National Climatic Data Center (NCDC) database updated the records for the latter datasets to the end of 2000 through the beginning of 2001. Monthly SLP for western land stations have been obtained from the University Corporation for Atmospheric Research (UCAR), the EOS DAAC, and NCDC databases. SAT and SLP data from Russian NP stations are available on CD-ROM from the NSIDC. The NP stations were continuously maintained from 1950 to 1991, with one to three stations operating at any given time. These observations are considered the most accurate for SAT in the Arctic Ocean (Rigor et al. 2000). Monthly gridded drifting buoy data for 1979–98 were obtained from the Polar Science Center of the University of Washington. Additionally, reanalysis data has been used to evaluate the spatial patterns of SAT and SLP. The SLP reanalysis data were obtained from the National Center for Atmospheric Research (NCAR; 1990) CD-ROM. Daily (National Centers for Environmental Prediction) NCEP–NCAR reanalysis SAT were provided by the National Oceanic and Atmospheric Administration–Cooperative Institute for Research in Environmental Sciences (NOAA–CIRES) Climate Diagnostic Center in Boulder, Colorado. Note that for composite Arctic SAT and SLP time series we used data from stations northward of 62°N only, whereas in the correlation and other analyses more southern stations were included.

Historically, European countries have maintained good station coverage, providing the longest records of air temperature and pressure (Fig. 1). Meteorological observations over land regions of Russia and Alaska also have reasonable station coverage and length. A few long time records are also available from the Northwest Territories of Canada. In our analysis, we utilize the best 75 out of 200 available land stations, maintaining approximately homogeneous spatial coverage and omitting records with gaps. Twenty-four records are longer than 100 yr, and 31 other records are longer than 65 yr, while observations from 20 stations cover less than 65 yr. The shortest used record is 43 yr. To eliminate site
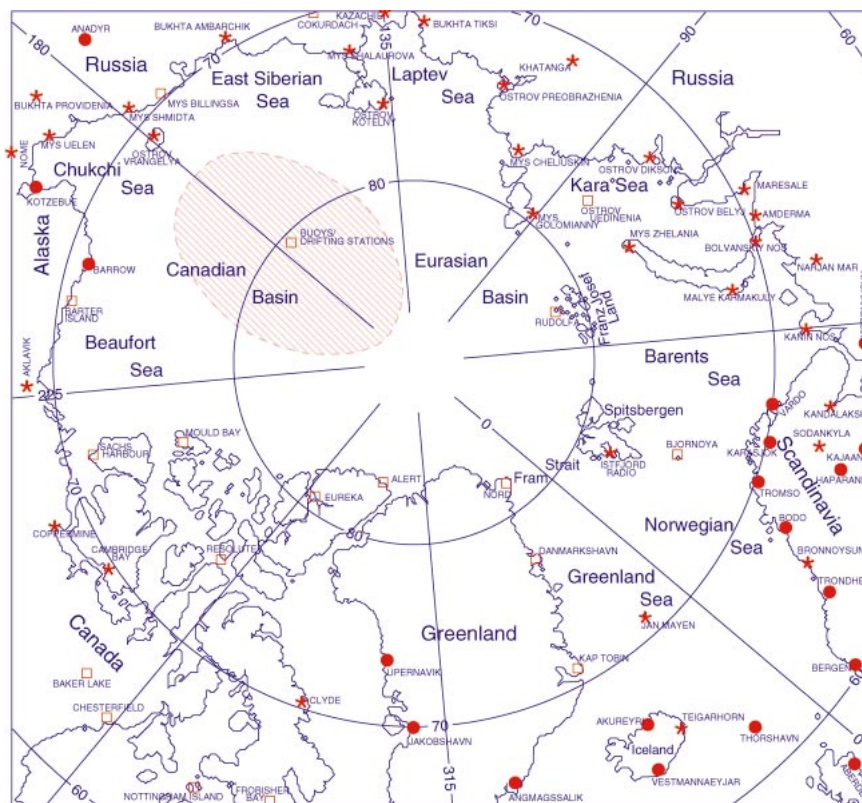
FIG. 1. The locations of SAT and SLP observations. Red circles show stations with $L \geq 100$ yr of observations, red stars represent stations with $65 \leq L < 100$ yr, and red squares indicate stations with $L < 65$ yr. The red cross-hatched oval denotes the region represented by data from the NP manned stations and IABP drifting buoys.

density bias, we omitted data before 1875 because only a few time records, mostly from Scandinavian stations, extend to earlier years. Fortunately, the remaining geographical bias in the early part of the composite time series is relatively small (Polyakov et al. 2002). All the land station data have been assessed for homogeneity using interstation comparisons [see discussion of homogeneity assessment techniques in Jones et al. (1999)]. Monthly data have also been assessed for errors by identifying peaks exceeding three standard deviations and then checking them with nearby station records.

The region in the Canadian Basin from where the NP and buoy data were collected is highlighted in Fig. 1 by a cross-hatched oval centered at 180°. This region was chosen because it contains the maximum density of NP stations. The size of the region is within the correlation length scale (CLS) introduced by Rigor et al. (2000) as a measure of how fast the SAT correlation decreases with distance. According to Rigor et al. (2000), a reasonable choice for the CLS is 900–1000 km for stations on the pack ice. A composite time series for SLP and SAT in the region for 1950–90 was constructed using the monthly data that were nearest the center of the NP region. SLP and SAT time series from the gridded IABP drifting buoy data for this same region

were used to cover the period 1979–98. The overlapping period from these two datasets from 1979 to 1990 has been used to check the consistency between NP and buoy data. We compared monthly temperature and pressure from the NP stations with buoy observations interpolated to the location of the NP stations. On average, there was not a substantial bias in summer SAT between these two datasets because the buoy data have been previously filtered to match the statistics of the NP observations (Rigor et al. 2000). However, we found rather large differences in temperatures for the cold season (October–April) with an average bias of 1.5°C (buoy SAT was warmer). We also found a slight, up to 0.5 mb, bias for the SLP records. These biases were removed from the buoy data before using these data to extend the NP region SAT and SLP time series to 1998.

The goal of creating this dataset was to obtain a single time record for monthly SAT and SLP, which could elucidate the entire Arctic and sub-Arctic air temperature and pressure variability. Following Chapman and Walsh (1993) and Jones et al. (1999), the record from each station was reduced to monthly anomalies relative to 1961–90 (note that the computed trends are somewhat sensitive to the reference period used for calculation of anomalies). The anomalies for all available stations were
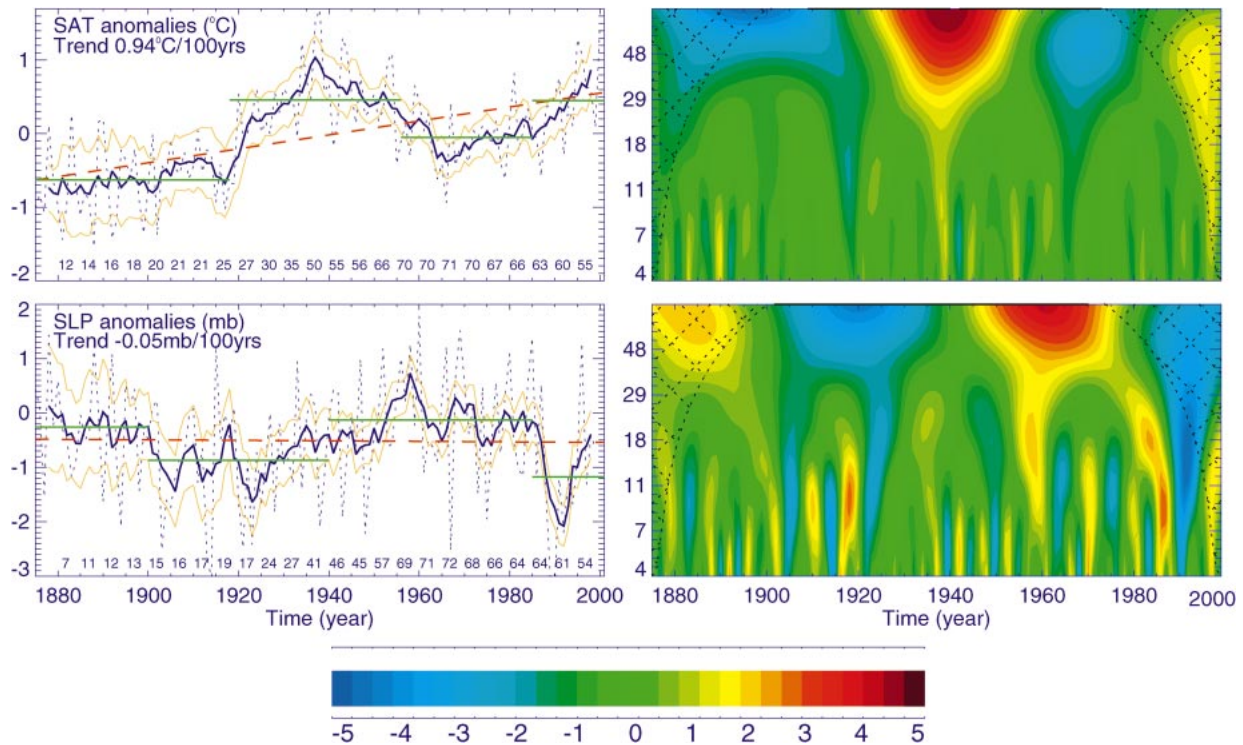
FIG. 2. (top left) Composite time series of the annual SAT (°C), and (bottom left) SLP (mb) anomalies for the region poleward of 62°N. Blue dashed lines show annual means, blue solid lines 6-yr running means and the yellow lines their 95% confidence intervals. Red dashed lines show trends, and green horizontal lines show means for positive and negative LFO phases. Numbers in the bottom parts of the panels show the number of stations used for averaging. (top right) Wavelet transform of monthly air temperature and (bottom right) pressure using the Mexican hat ($m = 2$) wavelet (Torrence and Compo 1998). Vertical axes show the period in years. Cross-hatched areas denote the region of the wavelet spectrum in which edge effects are important.

then averaged. The central Arctic might be underrepresented, having been described by a single time series from drifting NP buoys. To assure that this is not the case, we also used a technique similar to the climate anomaly method (CAM) described by Jones et al. (1999). In this method, the total area is divided into boxes, and anomaly time series are averaged within each box. The resulting average time series for each grid box are averaged again to obtain a single "global" time series. In our case, individual records from land stations over 10 regions were averaged to produce 10 time series. Each of the 10 averaging areas was approximately equal to the region from the central Arctic Ocean marked by red cross-hatching in Fig. 1. The resulting records, plus those obtained from the drifting NP buoys, were averaged to produce the final record for the entire circum-Arctic northward of 62°N. Upon comparison, the difference between the two resulting time series (obtained from simple averaging of all available records and by the CAM method) is insignificant (for SAT, the correlation is 0.95, and the standard deviations are 0.66 and 0.67). Trends in the final time series of monthly temperature and pressure were evaluated by the least squares best-fit method.

3. Low-frequency variability

The composite time series of the air temperature and pressure anomalies for the Arctic and sub-Arctic are shown in Fig. 2. In analyzing hemispheric and global temperatures, Jones et al. (1999) documented two distinct warming periods from 1920 to 1945, and from 1975 to the present. The same periods stand out for the 55°–85°N zonal band (Serreze et al. 2000) and for the circum-Arctic region northward of 62°N (this study, Fig. 2). In contrast to the global and hemispheric temperature rise, the high-latitude temperature was higher in the late 1930s through the early 1940s than in recent decades. The magnitude of these maxima was almost indistinguishable within the 55°–85°N zonal band (Serreze et al. 2000) whereas northward of 62°N the 1938 maximum of annual Arctic SAT anomaly reached 1.69°C compared with the 2000 maximum of 1.49°C. This difference appears to be governed by a much steeper high-latitude SAT rise in the 1920s–30s.

The SAT time series appears to exhibit two negative (cold) and two positive (warm) phases of multidecadal variability at a timescale of 50–80 yr [low-frequency oscillation (LFO), Polyakov and Johnson (2000)] superimposed on a background warming trend. The SLP
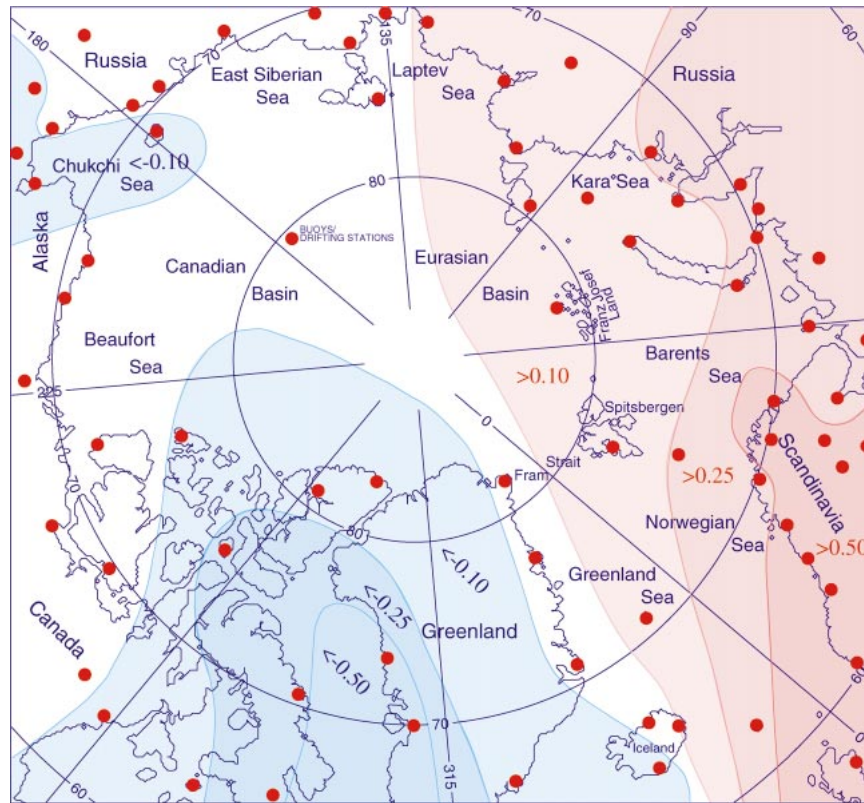
Fig. 3. Correlations between the monthly NAO index and SATs from coastal stations. Only statistically significant (95% level) correlations are presented.

time series also shows signs of multidecadal variability with generally higher values before 1900 and between the 1940s and mid-1980s (negative LFO phases) and lower values between 1900 and the 1930s and from the mid-1980s to the present (positive LFO phases).

The LFO is evident in various instrumental and proxy records of the Northern Hemisphere (Schlesinger and Ramankutty 1994; Minobe 1997; Mann et al. 1995). Proxy-based SAT reconstructions for the past 330 yr show a mode of variability at approximately 70 yr (Delworth and Mann 2000). Observations display distinct basinwide patterns of multidecadal SST variability centered in the North Atlantic. The SST anomalies appear to maintain large-scale SLP anomalies (Deser and Blackmon 1993; Kushnir 1994; Mann and Park 1996; Delworth and Mann 2000). The variability has a high degree of Arctic (Vinnikov et al. 1980; Polyakov et al. 2002) and some degree of global (Schlesinger and Ramankutty 1994) expression. An analysis of a long-term integration of the Geophysical Fluid Dynamics Laboratory coupled atmosphere–ocean model, suggests that this variability is related to fluctuations in the thermohaline circulation in the North Atlantic (Delworth and Mann 2000). Polyakov et al. (2002), using an extended 1875–2001 Arctic SAT record, also demonstrated stronger multidecadal variability in the polar region compared with the lower latitudes. This may suggest that

the origin of this variability may be hidden in complex interactions between the Arctic and North Atlantic. This suggestion is supported by the correlations between air temperature from Arctic coastal stations and the North Atlantic Oscillation (NAO) index, which is characterized by a north–south-oriented dipole in sea level pressure structure over the Atlantic. Maximum correlations are found in the near-Atlantic region, and the correlations decay toward the North Pacific (Fig. 3).

The wavelet transform of the SAT and SLP time series displays strong low-frequency variability on the decadal and interdecadal timescales with the strongest signal at LFO periods (Fig. 2, right). The Arctic SAT wavelet transform is qualitatively similar to that of the global air temperature analyzed by Lau and Weng (1995). The wavelet analysis provides evidence of the evolutive spectrum of the SAT and SLP variability when the LFO frequency is different in time with shorter LFO phases by the end of the records. The higher temperatures in the Arctic in the 1930s–40s and in the recent decades, and the lower temperatures in the 1960s–70s and prior to the 1920s may be associated, at least partly, with the positive and negative phases of the LFO. Generally, negative, anticyclonic LFO phases in SLP are associated with lower air temperatures, whereas positive, cyclonic LFO phases in SLP have higher temperatures (Polyakov and Johnson 2000). However, the LFO phases in the
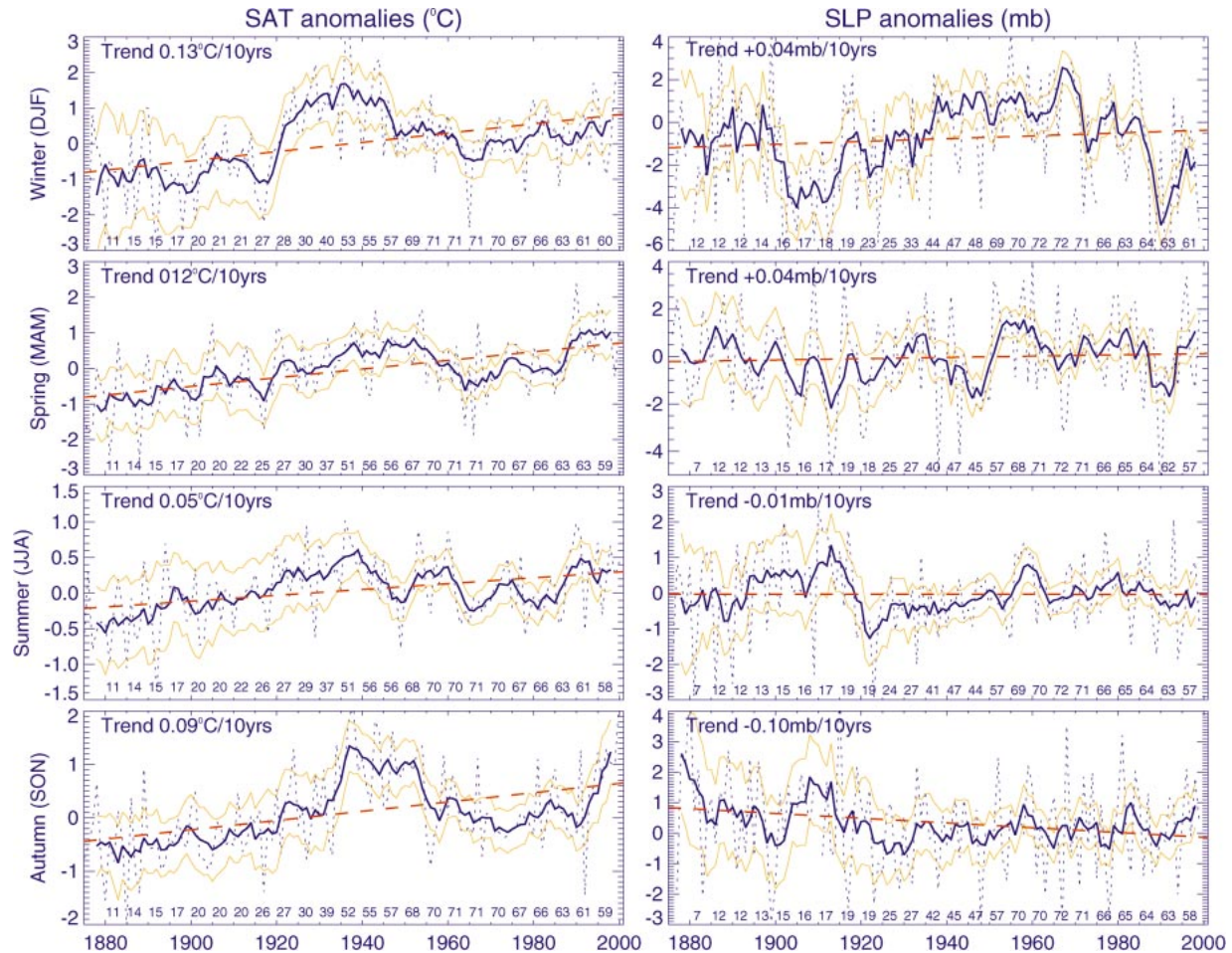
FIG. 4. As the left side of Fig. 2, but for (left) seasonal temperature and (right) pressure anomalies. Note that the vertical scale varies with season.

SAT record lag those from the SLP record by about 5–15 yr, implying that the physics associated with this low-frequency variability is complicated. (Note that different time periods of SAT and SLP have been used to construct the spatial patterns in Fig. 5 to account for this phase difference.)

The multidecadal Arctic SAT and SLP variability expresses strong seasonality being particularly strong in cold season but much weaker during the warm season (Fig. 4). Mann and Park (1996) analyzed seasonal expressions of the SLP and sea surface temperatures (SST) multidecadal variations in the Northern Hemisphere. They found a significant impact of North Atlantic circulation during the cold season on Eurasian temperatures. Strong coupling between the Arctic and North Atlantic suggests that the cold-season expression of the arctic LFO may be modulated by the North Atlantic processes.

The seasonal differences in alternate warming periods (1920s–30s and from the 1980s to the present) and cooling period (1940s–50s) are striking. For example, the warming in the 1920s–30s was rapid in spring and au-

tumn and very rapid in winter, and was much weaker in summer. The period from 1918 to 1922 displays exceptionally rapid winter warming not only in the circum-Arctic region northward of 62°N but also in the 55°–85°N zonal band (Serreze et al. 2000, their Fig. 3). The autumnal rapid temperature rise in the 1930s was local and was observed in Scandinavia and the western part of maritime Russia only. The warming of the 1980s–90s was exceptionally strong in the spring and autumn, while the winter and summer temperature increase was relatively moderate. The spatial pattern and timing of warming during the 1990s are in general agreement with the results of Chapman and Walsh (1993) and Rigor et al. (2000). However, our SAT record does not show particularly strong winter warming in the central Arctic due to, perhaps, positive SAT winter bias, which is removed from the buoy data.

Figure 5 displays the NCAR reanalysis SLP fields averaged over the positive (1986–97) and negative (1946–85) LFO phases. It shows that during the negative LFO phase, the center of high SLP in the western Arctic is well developed and the Icelandic low is depressed,
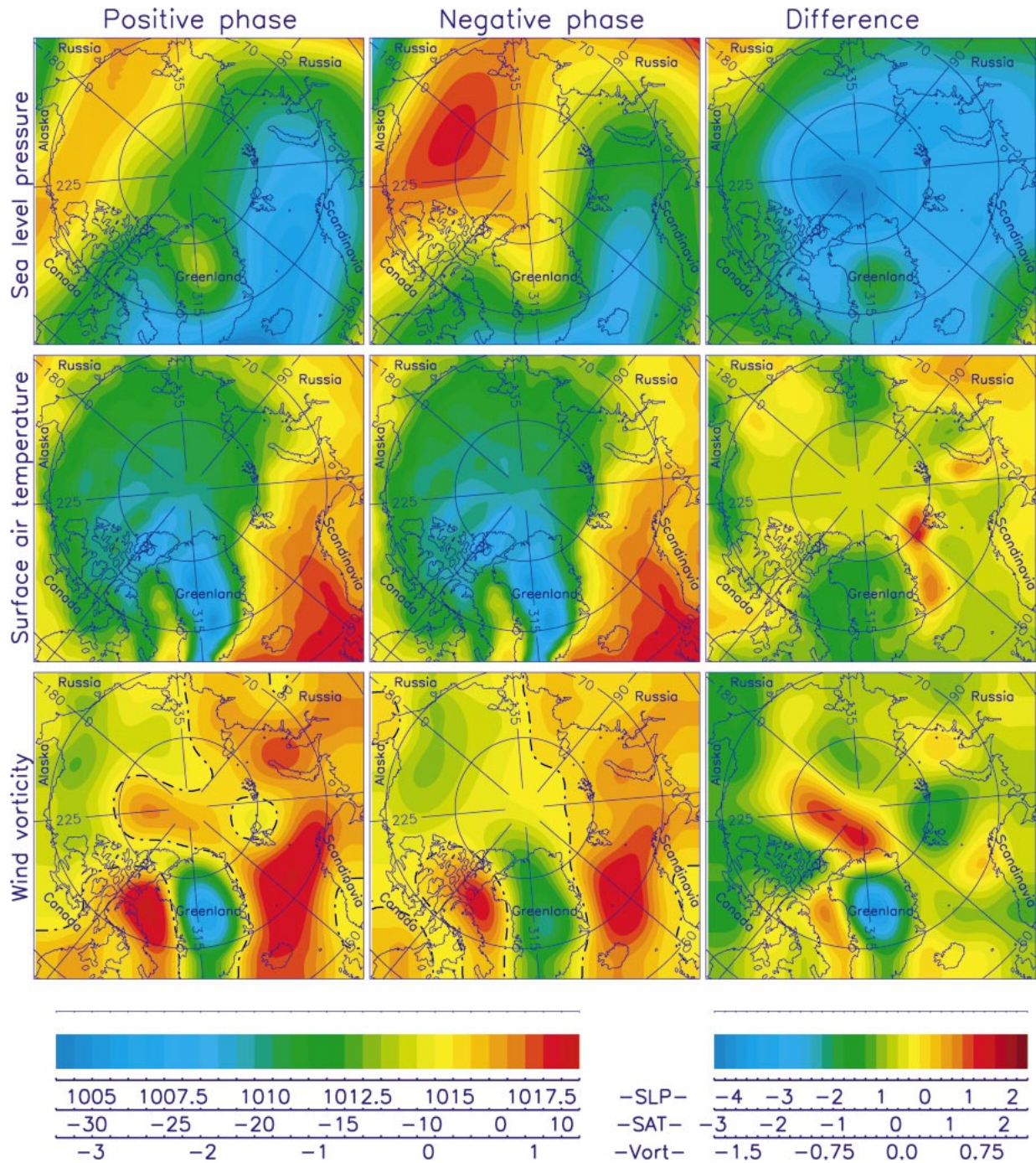
FIG. 5. (top) NCAR SLP (mb), (middle) NCEP–NCAR SAT (°C), and (bottom) wind vorticity (mb) computed from the NCAR SLP. The left (center) panels show the averages for the positive (negative) phases of the LFO, and the right panels show the difference between the positive and the negative phase.

while during the positive LFO phase, the SLP high in the western Arctic is weaker and the Icelandic low is deeper and extends farther into the Barents and Kara Seas. The zonally symmetric cells of SLP difference between the two LFO phases bear a strong resemblance to the decadal SLP pattern found by Johnson et al. (1999), to the difference of the 8-yr mean patterns for 1979–86 and 1987–94 shown by Walsh et al. (1996), and the Arctic Oscillation (AO) pattern described by Thompson and Wallace (1998). The SAT derived from the NCEP–NCAR reanalysis data (Fig. 5) covaries with the LFO phases, with higher overall air temperatures in

the central Arctic, Greenland Sea, central Russia, and east of Novaya Zemlya in the Barents Sea during the positive LFO phases (1948–55 and 1986–97) than during negative phases (1956–85). However, the NCEP reanalysis air temperature fields show cooling in the Laptev Sea region and over eastern Siberia, which is not supported by direct observations (Chapman and Walsh 1993; Jones et al. 1999; Rigor et al. 2000). SAT fields composed from our dataset, based on land stations, the North Pole (NP), and drifting buoy records (not shown) indicate overall higher temperatures during the positive LFO phases compared with the negative LFO phases (including the Laptev Sea and Siberia regions where the NCEP data shows the opposite tendency).

Gudkovich (1961) suggested that the Arctic atmospheric circulation alternates between regimes with a weakened/strengthened anticyclonic Beaufort gyre, and intensified/suppressed cyclonic circulation in the eastern Arctic. Polyakov and Johnson (2000) found that this pattern is typical for both decadal variability and the multidecadal LFO (see their Fig. 4). In this dipolelike structure a zero vorticity contour separates two large-scale centers of atmospheric circulation. During the anticyclonic regime of the LFO, or a decadal fluctuation, this contour goes roughly from the Laptev Sea to the Eurasian Basin and farther toward the Fram Strait (Fig. 5, bottom panels, dot–dash line). During the cyclonic regime of LFO or decadal fluctuation this boundary is shifted eastward. Walsh et al. (1996), analyzing decadal variability, demonstrated a shrinking of the Beaufort gyre since the late 1980s. Maslanik et al. (1996) found substantially greater cyclonic activity for years associated with the positive (1988–93) as compared to the negative (1982–87) phase of the decadal mode of variability identified by Proshutinsky and Johnson (1997). The eastward shift of the zero-vorticity contour took place in the western Arctic during the positive phase of LFO and in the eastern Arctic during the positive phase of the decadal fluctuation.

These changes in atmospheric circulation have a profound effect on the Arctic ice conditions. For example, Proshutinsky and Johnson (1997) found periods of intensified cyclonic–anticyclonic ice drift to be associated with decadal cyclonic–anticyclonic atmospheric circulation regimes. Walsh et al. (1996) argued that cyclonic winds cause divergent ice drift resulting in overall thinner ice while anticyclonic winds produce convergent ice motion and generally thicker ice. Polyakov et al. (1999) found that cyclonic atmospheric circulation regimes associated with increased atmospheric vorticity favor cyclonic ice drift and lighter ice conditions, while anticyclonic regimes with decreased atmospheric vorticity result in anticyclonic ice motion and generally thicker ice in the eastern Arctic. Steele and Boyd (1998) demonstrated an eastward shift of the zero contour of sea ice vorticity from the mid-1980s to the late 1980s and 1990s. Polyakov and Johnson (2000) found the multidecadal LFO and decadal fluctuations to drive the Arctic

basinwide ice volume variability. Zhang et al. (2000) also found a dependence of ice variability on the strength of the NAO. Figure 5 corroborates these findings by showing a substantial LFO-driven increase of wind vorticity in the western Arctic in the 1980s–90s. This area approximately matches the western part of the Scientific Ice Expeditions (SCICEX) region where Rothrock et al. (1999) found a decrease in Arctic ice thickness by about 0.9–1.4 m in the mid-1980s–90s relative to the 1950s–70s. Note that the decadal mode of variability in this Arctic region showed a slight increase of wind anticyclonicity in the 1990s (Maslanik et al. 1996), which would actually reduce LFO-driven ice decay there. This implies that the recent LFO-driven change of wind pattern from anticyclonic to cyclonic accounts for the observed reduction of ice thickness in the western Arctic.

4. Trends

The composite time series of the air temperature and pressure anomalies for the Arctic and sub-Arctic region (Fig. 2) are used to evaluate SAT and SLP trends. The SLP displays strong variability with a negligible background trend of -0.005 mb decade^{-1}. Since 1875 Arctic air temperature shows warming with an average rate of $0.09°C$ decade^{-1} (Fig. 2). The warming occurs over all seasons, being greatest in winter [December–January–February (DJF)] and spring [March–April–May (MAM)] ($0.13°$ and $0.12°C$ decade^{-1}, respectively; Fig. 4). The autumnal [September–October–November (SON)] rate was slightly lower ($0.09°C$ decade^{-1}). The SAT warming trend was weakest in summer [June–July–August (JJA)], with a rate of $0.05°C$ decade^{-1}. These seasonal differences are qualitatively consistent with those from Jones et al. (1999) for global and hemispheric trends and with the $55°–85°N$ zonal band seasonal air temperature trends documented by Serreze et al. (2000). However, the rate of Arctic SAT increase in 1875–2001 is twofold compared with the Northern Hemisphere trend. Vinnikov et al. (1980) also found a twofold polar amplification of SAT trends for 1891–1978 (Table 1). Comparing SAT trends for 1901–97 (potentially the period with the most pronounced human impact) the difference between the Jones et al. (1999) Northern Hemisphere data and Arctic data is only $0.01°C$ decade^{-1} (Arctic trend < Northern Hemispheric trend), a statistically indistinguishable 20% difference (Table 1). Polyakov et al. (2002) argued that the similarity of century-long Arctic and Northern Hemisphere air temperature trends may result from near-cancellation of positive/negative LFO phases and does not support amplified warming in polar regions as predicted by GCMs (Houghton et al. 2001). Przybylak (2000), analyzing Arctic SAT, also underlined this inconsistency.

Strong multidecadal variability in SAT and SLP records results in an oscillatory behavior of air temperature and pressure trends (Fig. 6). For example, during

TABLE 1. Trends of air temperature (°C decade^{-1}) from various sources.

Source	Region	Period	Trend	Trend from this study poleward of 62°N
Vinnikov et al. (1980)	17.5°–87.5°N	1891–1978	+0.04	
	72.5°–87.5°N	1891–1978	+0.07	+0.09 ± 0.05
	72.5°–87.5°N	1940–64	−0.56	−0.25 ± 0.29
Chapman and Walsh (1993)	Land stations	1961–90	+0.19	+0.17 ± 0.18
Kahl et al. (1993)	Arctic Ocean	1950–90	−0.37	−0.05 ± 0.13
Martin et al. (1997)	Central Arctic Ocean	1961–90	+0.14	+0.17 ± 0.18
Jones et al. (1999)	Northern Hemisphere	1861–1997	+0.04	
	Northern Hemisphere	1901–97	+0.06	+0.05 ± 0.04
Rigor et al. (2000)	Eastern Arctic Ocean	1979–97	+1.00	
	Western Arctic Ocean	1979–97	+0.00	
Present study	Poleward of 62°N	1875–2000	+0.09 ± 0.03	

the previous 60 yr (i.e., since the 1940s) the Arctic SAT trend was positive. However, Arctic temperatures in the 1930s–40s were exceptionally high, so that from the 1920s forward the data have a small but statistically significant cooling tendency. Extending the time series further back into the nineteenth century, the temperature trend again changes sign, signifying a general warming tendency over the entire record. Moreover, over the 125-yr Arctic SAT record Polyakov et al. (2002) identified periods when Arctic trends were actually smaller or of different sign than Northern Hemisphere trends. Computed Arctic SAT trends depend on the phases and intensity of the LFO in addition to any long-term underlying trend, whereas Northern Hemisphere trends do not show such a strong dependence on the LFO. The SLP trend also shows an oscillatory behavior, but the change of sign by the SLP trend is not statistically significant. Another illustration of oscillatory LFO-dependent behavior of the SAT trend is a strong cooling of −0.25°C decade^{-1} associated with the downward slope of the positive LFO phase in the period 1940–64 (Table 1), which is consistent in sign but somewhat weaker than the Vinnikov et al. (1980) trend of −0.56°C decade^{-1}. This analysis underscores the inherent difficulty in dif-

ferentiating between trends and long-term fluctuations (see also Ghil and Vautard 1991).

Trends in Arctic SAT for the recent decades have been discussed in several studies and vary between −0.37° and +0.19°C decade^{-1} in part due to different periods analysed (Table 1). Chapman and Walsh (1993) examined SAT using Arctic land stations observations for 1960–90, whereas Martin et al. (1997) analyzed temperatures over the pack ice for the same period. These estimates are relatively close and show warming trends of 0.19° and 0.14°C decade^{-1}, respectively. These trends are also consistent with ours of 0.17°C decade^{-1} calculated for the same period of time. Kahl et al. (1993) analyzed temperatures measured over the central Arctic Ocean in the 1950s–90s using radiosonde observations from NP stations and dropsonde observations from the United States Air Force "Ptarmigan" weather reconnaissance program. In contrast to other studies, they detected strong cooling trends in Arctic air temperatures. Discussing these controversial results, Jones et al. (1999) suggest that this discrepancy may be due to long instrumental time lags of the dropsonde or to a geographical bias of dropsonde observations compared with NP radiosonde measurements. We found negative (although weaker) SAT trends from our record for 1950–90 as well (see Table 1). Thus, extending our time record for an additional 11 yr beyond 1961 results in a change of the sign of SAT trend from positive (warming) to negative (cooling), in qualitative agreement with the findings of Kahl et al. (1993). The above inconsistencies in Arctic SAT trends may be partly explained in the context of the mid-1960s minimum in LFO.

5. Conclusions

We examine Arctic surface air temperature and pressure data for the period 1875–2000 using long-term records from the maritime Arctic, poleward of 62°N. Arctic air temperature and pressure display substantial variability on timescales of 50–80 yr. The multidecadal variability (LFO) is evident in various instrumental and proxy records for the Northern Hemisphere. This variability appears to originate in the North Atlantic and
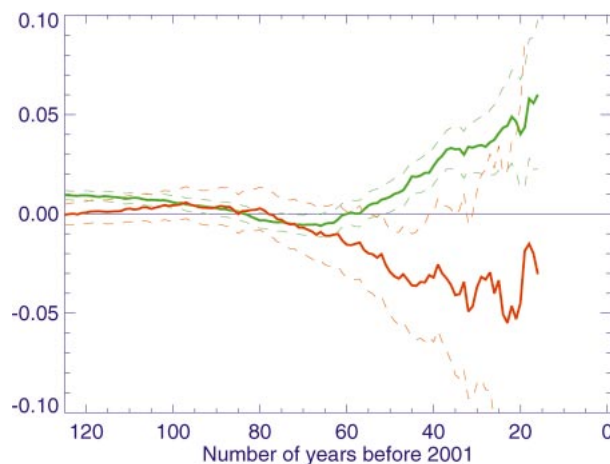

FIG. 6. SAT (°C yr^{-1}, green) and SLP (mb yr^{-1}, red) trends (solid lines) and their 95% confidence intervals (dashed lines).

is likely induced by slow changes in oceanic thermohaline circulation (Delworth and Mann 2000). However, SAT records demonstrate stronger multidecadal variability in the polar region than in lower latitudes. This may suggest that the origin of this variability may lie in the complex interactions between the Arctic and North Atlantic. Associated with the LFO, the SAT record shows two periods with the highest temperatures in the Arctic: in the 1930s–40s, and in recent decades. In contrast to the global and hemispheric temperature, the maritime Arctic temperature was higher in the late 1930s through the early 1940s than in the 1980s–90s.

The composite temperature record shows that since 1875 the Arctic has warmed by 1.2°C, so that over the entire record the warming trend was 0.094°C decade^{-1}, with stronger spring- and wintertime warming. The Arctic temperature trend for the twentieth century (0.05°C decade^{-1}) was close to the Northern Hemispheric trend (0.06°C decade^{-1}). The oscillatory behavior of Arctic trends results from incomplete sampling of the large-amplitude LFO. For example, the Arctic temperature was higher in the 1930s–40s than in recent decades, and hence a trend calculated for the period 1920 to the present actually shows cooling. Enhancement of computed trends in recent decades can be partially attributed to the current positive LFO phase.

We speculate that warming alone cannot explain the retreat of Arctic ice observed in the 1980s–90s. Also crucial to this rapid ice reduction was the low-frequency shift in the atmospheric pressure pattern from anticyclonic to cyclonic. Positive and negative LFO phases of the SAT are shifted by 5–15 yr relative to those in the SLP record. The complicated nature of Arctic temperature and pressure variations makes understanding of possible causes of the variability, and evaluation of the anthropogenic warming effect most difficult.

REFERENCES

Aleksandrov, Ye. I., and A. A. Dementyev, 1995: Surface meteorological database of polar regions and its use. *Formation of a Sea Ice and Hydrometeorology Database,* HydroMeteoIzdat, 67–75.

Cess, R. D., and Coauthors, 1991: Interpretation of snow–climate feedback as produced by 17 general circulation models. *Science,* **253,** 888–892.

Chapman, W. L., and J. E. Walsh, 1993: Recent variations of sea ice and air temperature in high latitudes. *Bull. Amer. Meteor. Soc.,* **74,** 33–47.

Crowley, T. J., 2000: Causes of climate change over the past 1000 years. *Science,* **289,** 270–277.

Cubasch, U., R. Voss, G. C. Hegerl, J. Wazskewitz, and T. J. Crowley, 1997: Simulation of the influence of solar radiation variations on the global climate with an ocean–atmosphere general circulation model. *Climate Dyn.,* **13,** 757–767.

Delworth, T. L., and T. R. Knutson, 2000: Simulation of the early 20th century global warming. *Science,* **287,** 2246–2250.

——, and M. E. Mann, 2000: Observed and simulated multidecadal variability in the Northern Hemisphere. *Climate Dyn.,* **16,** 661–676.

——, S. Manabe, and R. J. Stouffer, 1993: Interdecadal variations of the thermohaline circulation in a coupled ocean–atmosphere model. *J. Climate,* **6,** 1993–2011.

Deser, C., and M. Blackmon, 1993: Surface climate variations over the North Atlantic Ocean during winter: 1900–89. *J. Climate,* **6,** 1743–1753.

Gates, W. L., and Coauthors, 1996: Climate models—Evaluation. *Climate Change 1995,* J. T. Houghton et al., Eds., Cambridge University Press, 233–284.

Ghil, M., and R. Vautard, 1991: Interdecadal oscillations and the warming trend in global temperature time series. *Nature,* **350,** 324–327.

Gudkovich, Z. M., 1961: Relationship between ice drift in the Arctic Basin and ice conditions in the Soviet Arctic Seas. *Trans. Oceanogr. Committee,* **11,** 13–20.

Houghton, J. T., Y. Ding, D. J. Griggs, M. Noguer, P. J. van der Linden, and D. Xiaosu, Eds., 2001: *Climate Change 2001: The Scientific Basis.* Cambridge University Press, 944 pp.

Johnson, M. A., and I. V. Polyakov, 2001: The Laptev Sea as a source for recent Arctic Ocean salinity changes. *Geophys. Res. Lett.,* **28,** 2017–2020.

——, A. Y. Proshutinsky, and I. V. Polyakov, 1999: Atmospheric patterns forcing two regimes of arctic circulation: A return to anticyclonic conditions? *Geophys. Res. Lett.,* **26,** 1621–1624.

Jones, P. D., M. New, D. E. Parker, S. Martin, and I. G. Rigor, 1999: Surface air temperature and its changes over the past 150 years. *Rev. Geophys.,* **37,** 173–199.

Kahl, J. D., D. J. Charlevoix, N. A. Zaitseva, R. C. Schnell, and M. C. Serreze, 1993: Absence of evidence for greenhouse warming over the Arctic Ocean in the past 40 years. *Nature,* **361,** 335–337.

Kushnir, Y., 1994: Interdecadal variations in North Atlantic sea surface temperature and associated atmospheric conditions. *J. Climate,* **7,** 141–157.

Lau, K.-M., and H. Weng, 1995: Climate signal detection using wavelet transform: How to make a time series sing. *Bull. Amer. Meteor. Soc.,* **76,** 2391–2402.

Manabe, S., and R. J. Stouffer, 1994: Multiple-century response of a coupled ocean–atmosphere model to an increase of atmospheric carbon dioxide. *J. Climate,* **7,** 5–23.

Mann, M. E., and J. Park, 1996: Joint spatiotemporal modes of surface temperature and sea level pressure variability in the Northern Hemisphere during the last century. *J. Climate,* **9,** 2137–2162.

——, ——, and R. S. Bradley, 1995: Global interdecadal and century-scale oscillations during the past five centuries. *Nature,* **378,** 266–270.

Martin, S., E. A. Minoz, and R. Drucker, 1997: Recent observations of a spring–summer surface warming over the Arctic Ocean. *Geophys. Res. Lett.,* **24,** 1259–1262.

Maslanik, J. A., M. C. Serreze, and R. G. Barry, 1996: Recent decreases in Arctic summer ice cover and linkages to atmospheric circulation anomalies. *Geophys. Res. Lett.,* **23,** 1677–1680.

Minobe, S., 1997: A 50–70 year climatic oscillation over the North Pacific and North America. *Geophys. Res. Lett.,* **24,** 683–686.

Overpeck, J., and Coauthors, 1997: Arctic environmental change of the last four centuries. *Science,* **278,** 1251–1256.

Parkinson, C. L., D. J. Cavalieri, P. Gloersen, H. J. Zwally, and J. C. Comiso, 1999: Arctic sea ice extents, areas, and trends, 1978–1996. *J. Geophys. Res.,* **104,** 20 837–20 856.

Polyakov, I., and M. A. Johnson, 2000: Arctic decadal and interdecadal variability. *Geophys. Res. Lett.,* **27,** 4097–4100.

——, A. Yu. Proshutinsky, and M. A. Johnson, 1999: Seasonal cycles in two regimes of Arctic climate. *J. Geophys. Res.,* **104,** 25 761–25 788.

——, and Coauthors, 2002: Observationally based assessment of polar amplification of global warming. *Geophys. Res. Lett.,* **29,** 1878, doi:10.1029/2001GL011111.

Proshutinsky, A. Yu., and M. A. Johnson, 1997: Two circulation regimes of the wind-driven Arctic Ocean. *J. Geophys. Res.,* **102,** 12 493–12 514.

Przybylak, R., 2000: Temporal and spatial variation of surface air temperature over the period of instrumental observations in the Arctic. *Int. J. Climatol.,* **20,** 587–614.

Rigor, I. G., R. L. Colony, and S. Martin, 2000: Variations in surface air temperature observations in the Arctic, 1979–97. *J. Climate,* **13,** 896–914.

Rothrock, D. A., Y. Yu, and G. A. Maykut, 1999: Thinning of the arctic sea-ice cover. *Geophys. Res. Lett.,* **26,** 3469–3472.

Schlesinger, M. E., and N. Ramankutty, 1994: An oscillation in the global climate system of period 65–70 years. *Nature,* **367,** 723–726.

Serreze, M. C., F. Carse, R. G. Barry, and J. C. Rogers, 1997: Icelandic low cyclone activity: Climatological features, linkages with the NAO, and relationships with recent changes in the Northern Hemisphere circulation. *J. Climate,* **10,** 453–464.

——, and Coauthors, 2000: Observational evidence of recent change in the northern high-latitude environment. *Climatic Change,* **46,** 159–207.

Shindell, D. T., G. A. Schmidt, M. E. Mann, D. Rind, and A. Wapple, 2001: Solar forcing of regional climate change during the Maunder minimum. *Science,* **294,** 2149–2152.

Steele, M., and T. Boyd, 1998: Retreat of the cold halocline layer in the Arctic Ocean. *J. Geophys. Res.,* **103,** 10 419–10 435.

Stott, P. A., S. F. B. Tett, G. S. Jones, M. R. Allen, J. F. B. Mitchell, and G. J. Jenkins, 2000: External control of 20th century temperature by natural and anthropogenic forcings. *Science,* **290,** 2133–2137.

Thompson, D. W. J., and J. M. Wallace, 1998: The Arctic Oscillation signature in the wintertime geopotential height and temperature fields. *Geophys. Res. Lett.,* **25,** 1297–1300.

Timmerman, A., M. Latif, R. Voss, and A. Grotzner, 1998: Northern Hemispheric interdecadal variability: A coupled air–sea mode. *J. Climate,* **11,** 1906–1931.

Torrence, C., and G. P. Compo, 1998: A practical guide to wavelet analysis. *Bull. Amer. Meteor. Soc.,* **79,** 61–78.

Vinnikov, K. Ya., G. V. Gruza, V. F. Zakharov, A. A. Kirillov, N. P. Kovyneva, and E. Ya. Ran'kova, 1980: Recent climatic changes in the Northern Hemisphere. *Sov. Meteor. Hydrol.,* **6,** 1–10.

Walsh, J. E., and R. G. Crane, 1992: A comparison of GCM simulations of Arctic climate. *Geophys. Res. Lett.,* **19,** 29–32.

——, W. L. Chapman, and T. L. Shy, 1996: Recent decrease of sea level pressure in the central Arctic. *J. Climate,* **9,** 480–486.

Waple, A. M., M. E. Mann, and R. S. Bradley, 2002: Long-term patterns of solar irradiance forcing in model experiments and proxy based surface temperature reconstructions. *Climate Dyn.,* **18,** 563–578.

Zhang, J., D. A. Rothrock, and M. Steele, 2000: Recent changes in Arctic sea ice: The interplay between ice dynamics and thermodynamics. *J. Climate,* **13,** 3099–3114.